Energy Equip. Sys./ Vol. 11/No. 1/March 2023/ 13-28

ENERGY EQUIPSYS

Energy Equipment and Systems

http://energyequipsys.ut.ac.ir
www.energyequipsys.com

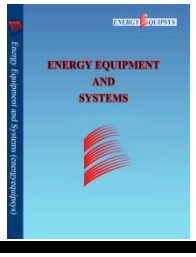

Numerical investigation on the performance of double pass two glazed solar air heaters with jet impingement

Authors

Seyyed Abdolreza Gandjalikhan Nassab [a*]

[a] School of Mechanical Engineering, College of Engineering, Shahid Bahonar University of Kerman, Kerman, Iran

Article history:
Received : 26 June 2022
Accepted : 2 September 2022

ABSTRACT

Solar air heaters are the simplest heat exchangers for converting solar irradiation into air enthalpy, but their efficiencies are low because the low density and heat capacity of the working fluid. To improve the performance, a new configuration of jet technique is proposed for heat transfer augmentation. The air jet streaks the heated absorber, which leads to extra turbulence and more rate of convection heat transfer. This technique is examined numerically here for the first time in a two-glazed double pass solar air heater by the Computational fluid dynamics simulation using the COMSOL Multiphysics. The hydrodynamic and thermal behavior of the heater is obtained by numerical solution of the continuity, momentum, and energy equations for both forced and free convection turbulent air flow based on the k–ε turbulence model. Also, the Laplace equation is solved for obtaining the temperature fields in solid elements. The performance of the proposed solar heater is investigated under different incoming solar heat flux and air mass flow rates. A significant increase in thermal efficiency for double pass solar air heaters with jet impinging technique is seen in comparison to conventional solar collectors. The maximum percentages of efficiency increase for the studied test cases are 10% and 6%, corresponding to 0.02 kg/s and 0.04 kg/s air mass flow rates, respectively.

Keywords: Jet Impingement, Double Pass SAH, Performance, Turbulent Flow.

1. Introduction

The freely available solar energy is one of the carbon-neutral sources, and solar air heaters (SAHs) are the heating thermal systems for converting thermal radiation into air enthalpy. These heat exchangers have many applications both in the industrial and agriculture sectors.

The design of more efficient solar collectors can be regarded as a step forward in using more clean solar energy. The use of SAHs in cooking technology was explained in the study by Aramesh et al. [1], and several other

* Corresponding author: S.Abdolreza Gandjalikhan Nassab
School of Mechanical Engineering, College of Engineering, Shahid Bahonar University of Kerman, Kerman, Iran
Email: ganj110@uk.ac.ir

engineering applications of these thermal systems were reported and discussed in a paper by Kaligirou [2]. Due to the low conduction and low density of air, and thereby low thermal efficiency, a great number of studies with improving methods are going on by putting a number of efforts into various enhancement techniques, including designing concave and convex airflow channels [3], employing a wire-mesh packed bed [4], using fins and extended surfaces with different shapes [5], introducing various air duct geometries [6], using radiating working gas in both single pass [7] and also double pass SAHs [8], employing vortex generation technique [9] and designing the converged shape of air ducts [10]. Recently, it is found that the rate of heat transfer between the heated absorber and airflow can be increased by jet impingement technique. In addition to applying this technique in solar collectors [11], these applications mainly include several other systems such as turbine blade cooling [12] and micro-electro-mechanical components [13].

Literature review show that the concept of jet impingement in SAH for enhancing convection heat transfer was first introduced and studied experimentally by Choudhury and Garg [14]. In that research work, the effects of many geometrical parameters, such as the diameter of air nozzle and spacing between nozzles, were examined. It was revealed that the performance of SAHs with jet impingement under all operating conditions is better than solar collectors without a jet plate. Later on, the efficiency of an unglazed air heater with a jet technique was examined by Belusko et al. [15] and it was seen that the efficiency of heater is affected considerably by the jet spacing as the significant factor. With both numerical and experimental approaches, Xing et al. [16] analyzed the thermal behavior of SAHs with the inline jet array, and the staggered jet array configurations and different performances were reported for each case. The design of SAHs with a single slot jet was modified by Zukowski [17] and the effects of Reynolds number and nozzle to absorber space on thermo-hydrodynamic characteristics of solar heaters with jet impingement were explored. The thermal and flow behaviors of a novel microjet solar heater were examined experimentally by Zukowski [18]. The studied thermal system comprised two separated parallel air ducts with triangular shapes. The thermal efficiency of the proposed heater was found in the range of 66% to 90%. In the study by Chauhan and Thakur [19], the effects of some important geometrical parameters on the performance of SAH with a jet plate were examined and the maximum augmentation in convection heat transfer of 2.7 times was reported due to the jet method. The preference selection index methodology was employed by Chauhan et al.[20] to compute the values of the optimum geometrical parameters for the collector with jet impingement. The well-known Taguchi method was used in that study and the optimum values of the jet diameter ratio were obtained under different operating conditions. Matheswaran et al. [21] performed exergy and energy analyses for both single and double duct SAH with jet impingement, and the exergic efficiency of 4.36% was reported under the optimum values of jet plate geometrical factors.

The thermal characteristics of a modified single nozzle SAH were analyzed numerically by Rajaseenivasan et al. [22]. The effects of geometrical factors like nozzle diameter and attacked angle were studied in that work. To study the effect of jet impingement on the thermal performance of SAHs, a three-dimensional CFD simulation has been carried out by Yadav and Saini [23] using the RNG k–ε turbulence model. The effects of jet diameter ratio and jet height ratio on the thermal behavior of solar collectors operating under different steady conditions were studied and considerable enhancement due to jet impingement was reported.

Aboghrara et al. [24], investigated the thermal efficiency and the air outlet temperature of SAH with a jet plate. Results showed that using a corrugated absorber plate in the construction of heaters with jet technique improves well the performance of solar collector, such that about 14% increase in thermal efficiency was observed as compared to the simple SAH.

Abd et al. [25] proposed a new model of an absorber plate with V-corrugated shape in the jet SAHs and a comparison was made with the simple heater without jet plate under the same

conditions. Results revealed that the jet SAH efficiency is considerably higher than the conventional solar collector by 11.5%, 11% and 9% for the air mass flow rates of 0.02, 0.015, and 0.01 kg/s, respectively.

Chauhan et al. [26] experimentally studied the jet SAHs to find the optimal design . The obtained findings revealed that the thermal efficiency of solar collectors increases due to air jet but the pumping power for convection airflow is also increased.

In the present work which is the continuation of the mentioned previous research works, the effect of jet technique on the thermal performance of double-pass two-glazed SAH is investigated for the first time. Regarding the construction of SAHs with jet impingement and noticing to the direction of incoming solar irradiation towards the thermal system, the jet plate must be located below the absorber, such that this heated element becomes more closed to the glass cover from which the main heat loss takes place. Considering this fact, it is expected that the two-glazed double pass heater that keeps the absorber plate away from the cold ambient is a good configuration that matches jet impingement. This is the novel feature of the present work that has not been suggested and studied. So, in this paper, the plane double pass SAH with a jet plate (Fig.1) is simulated by CFD technique based on the finite element method (FEM). Both free and forced convection air flows exist in the system, the first occurs between the two glass covers and the second in the heater air ducts. Also, the surface radiation between the glass covers, absorber, and the jet plate is also considered in the simulation. Several test cases with different air mass flow rates and also different solar irradiation are analyzed.

Nomenclature

A	Area (m^2)
b	Height (m)
C_p	Specific heat (kJ/kg K)
D_h	Hydraulic diameter (m)
h	Convection coefficient (W/m^2K)
k	Thermal conductivity ($Wm^{-1}K^{-1}$)
L	Length (mm)
$\dot{m}$	Mass flow rate (kg/s)
p	Pressure (Pa)
q	Heat flux (W/m^2)
Re	Reynolds number =$\rho\overline{V_{in}}D_h/\mu$
T	Temperature (K)
u	Velocity fluctuation (m/s)
U	Turbulent mean velocity (m/s)
(x, y)	Coordinate system(m)

Greek symbols

α_g	Glass absorptivity
ρ_g	Glass reflectivity
τ_g	Glass transmissivity
δ	Thickness (m)
ϵ	Turbulent dissipation (m^3/s^2)
μ	Kinematic viscosity (Pa.s)
ρ	Density (kg/m^3)
α	Thermal diffusivity (m^2/s^2)
K	Turbulence kinetic energy (m^2/s^2)
ε	Surface emissivity
ν	Kinematic viscosity (m^2/s)
η	Efficiency
β	Volumetric thermal expansion (1/K)

Subscript

abs	absorber
amb	ambient
in	inlet
out	outlet
eq	equivalent
ins	insulation
i, j	Indices
g	glass

Superscript

‘	fluctuation
-	average

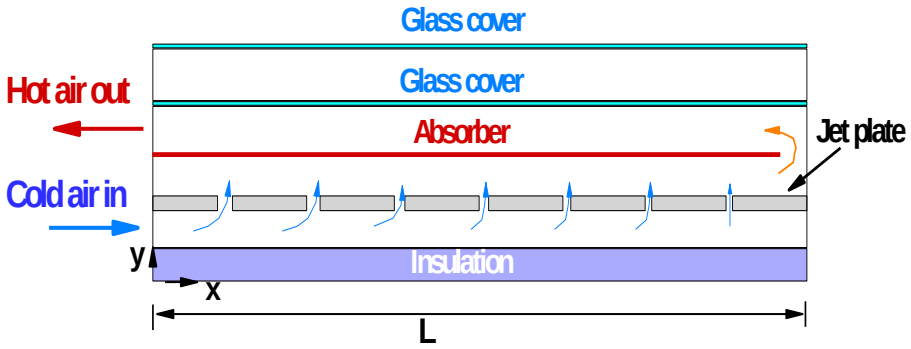

Fig. 1. Schematic of double pass SAH with impingement jet

2. Physical model

A schematic of the different parts of double pass SAH with two glass sheets is demonstrated in Fig.1. The heater length equals L=1 m, and all three air ducts where the forced convection airflow happens have the same height of b=4 cm. For air-forced convection, the Reynolds number which is defined as $\bar{V}D_h/\mu$, equals to 3800, corresponds to turbulent forced convection flow with the average velocity of $\bar{V}$ =0.7 m/s at the inlet section. The criteria of being laminar or turbulent for the free convection flow between two glasses is recognized based on the value of the Rayleigh number, $Ra=(g\beta\Delta Tb^3/\nu\alpha)=8700$, which also remains in the turbulent flow range with respect to the critical Rayleigh number of 1708 [27].

The CFD model of double pass two glazed SAH mainly consists of three rectangular ducts with a height of b=4 cm and length L=1m, seven holes on the jet plane with different widths, and the air gap between the two glass covers with a height b=4 cm. Choosing the holes with different widths is due to having almost equal air mass flow rate through each of them. For this purpose, the width of the first hole at the upstream side is 6.4 mm and this value 20% decreases towards the downstream side for subsequent holes. Also, the space between the center of each hole is equal to 12.5 cm and the first hole center is located at x= 16.7 cm. It should be noted that the values of these geometrical parameters were computed iteratively for having almost equal mass flow rates $m_{hole}=(m/7)$ with $\pm 5\%$ through each hole. A fully developed airflow is considered at the inlet section and two different air mass flow rates including 0.02 kg/s and 0.04 kg/s are assumed in the simulated test cases, corresponding to $\bar{V}=0.7\ and\ 0.35\ m/s$ at the inlet section. From the incoming uniformly distributed heat flux of q_{sun} =500 to 11000 W/ m^2 on the upper glass cover, equal to $\tau_g.\tau_g.q_{sun}$ reaches to the absorber plate.

2. 1. Governing equations

The set of equations for the simulation of air flows in jet SAH is presented in this section. Tow air flows exist inside the heater, the first is the forced convection turbulent airflow inside the heater's ducts and the second is the turbulent natural convection airflow because of the buoyancy effect inside the gap between the glass covers. Both flows are considered incompressible 2-D and steady. The forms of governing equations with tensor notations are given as follows:

$$\frac{\partial}{\partial x_i}(\rho U_i)=0 \tag{1}$$

$$U_j\frac{\partial(\rho U_i)}{\partial x_j}=-\frac{\partial p}{\partial x_i}+\frac{\partial}{\partial x_j}(\mu\frac{\partial U_i}{\partial x_j}-\rho\overline{u_iu_j})-\rho\beta g_i(T-T_{amb}) \tag{2}$$

$$U_j\frac{\partial(\rho T)}{\partial x_j}=\frac{\partial}{\partial x_j}(\frac{\mu}{\Pr}\frac{\partial T}{\partial x_j}-\rho\overline{Tu_j}) \tag{3}$$

The values of Reynolds stresses and turbulent heat fluxes are calculated by the following relations [28].

$$\overline{u_iu_j}=-\nu_t(\frac{\partial U_i}{\partial x_j}+\frac{\partial U_j}{\partial x_i})+\frac{2}{3}\kappa\delta_{ij} \tag{4}$$

$$\overline{Tu_j}=-\frac{\nu_t}{\Pr_t}\frac{\partial T}{\partial x_j} \tag{5}$$

$$\nu_t = C_\mu \frac{\kappa^2}{\varepsilon} \tag{6}$$

where, κ and ε, are calculated based of the following equations:

$$U_j \frac{\partial \kappa}{\partial x_j} = \frac{\partial}{\partial x_j}[(\nu + \frac{\nu_T}{\sigma_k})\frac{\partial \kappa}{\partial x_j}] + (P_k + G_k) - \varepsilon \tag{7}$$

$$U_j \frac{\partial \varepsilon}{\partial x_j} = \frac{\partial}{\partial x_j}[(\nu + \frac{\nu_T}{\sigma_\varepsilon})\frac{\partial \varepsilon}{\partial x_j}] + \frac{\varepsilon}{\kappa}[C_{\varepsilon_1}(P_k + G_k) - C_{\varepsilon_2}\varepsilon] \tag{8}$$

In Eqs. (7) and (8), G_b is the generation of kinetic energy by buoyancy and G_k is the kinetic energy generation due to the velocity gradient. The values of constant parameters in flow equations have been reported in Refs.[28] and [29]. It should be mentioned that the temperature-dependent density estimation and the buoyancy term in the y-momentum equation for free convection airflow are obtained by the Boussinesq approximation, such that this term is omitted from the momentum equation for the main forced convection airflow.

In the numerical model, a uniform heat flux is considered on the absorber plate due to the incoming solar irradiation, but the absorbed solar radiation inside the two glass covers that acts as an internal heat source is employed in the conduction equation for these solid parts. Therefore, in the computation of temperature distribution, the following equations are considered for the glass sheets.

$$\frac{\partial}{\partial x_j}(\frac{\partial T}{\partial x_j}) + \frac{q_{Sun}.\alpha_g}{k_g.\delta_g} = 0 \tag{9}$$

Also, for temperature computations of the absorber and jet plates, the following conduction equation is used:

$$\frac{\partial}{\partial x_j}(\frac{\partial T}{\partial x_j}) = 0 \tag{10}$$

The values of thermo-physical and radiative properties of solid elements used in the simulation are given in Table. 1.

2.2. Boundary conditions

The solutions of Eqs. (1) to (10) are carried out with appropriate boundary conditions which are tabulated in Table 2.

The values of heat transfer coefficients for the outer surfaces of the upper glass cover and the insulating layer are calculated using the following equations [29]:

$$h_{conv} = 5.67 + 3.68 V_{wind} \tag{11}$$

$$h_{rad} = \varepsilon_g \sigma \left(T_{g,t}{}^4 + T_{amb}{}^4\right)\left(T_{g,t} + T_{amb}\right) \tag{12}$$

In SAHs, the thermal efficiency shows the ability of the thermal system in converting solar radiation into gas enthalpy which is defined by the following relation:

$$\eta = \frac{\dot{m} C_p \left(T_{out} - T_{in}\right)}{\dot{q}_{sun} A} \tag{13}$$

3. Mesh study

Due to the rectangular shape of the studied SAH, the structured grid generation method was used with a refinement technique. Based on the grid study, five different mesh sizes were used in simulations. The corresponding maximum temperature that belongs to the absorber was calculated and the result is shown in Fig. 2. As seen, at 24100 nodes with a grid size of 312×77, the value of relative error falls below 1% , such that all simulations are performed based on this meshing as the optimum discretized domain.

Table 1. The solid elements' physical properties

Physical properties	Insulation	Glass covers	Absorber	Jet plate
Length [m]	1	1	0.96	1
Thickness[mm]	30	4	4	20
Conductivity [W/m.C]	0.04	0.8	400	400
Radiative emissivity	_	0.9	0.98	0.98
Radiative reflectivity	_	0.02	0.02	0.02
Radiative transmissivity	0	0.95	0	0

Table 2. Applied boundary conditions

Location	Condition
Top (Absorber)	Constant heat flux, No-slip
Top (Upper glass)	Convection with h_{eq}
Bottom (Insulation)	Convection with h_{eq}
Inlet section	Fully developed velocity inlet, T=T_{amb}, $\kappa = 0.005\bar{V}^2$
Outlet section	Pressure outlet
Air-solid interfaces	Continuity of temperature and heat flux, No-slip

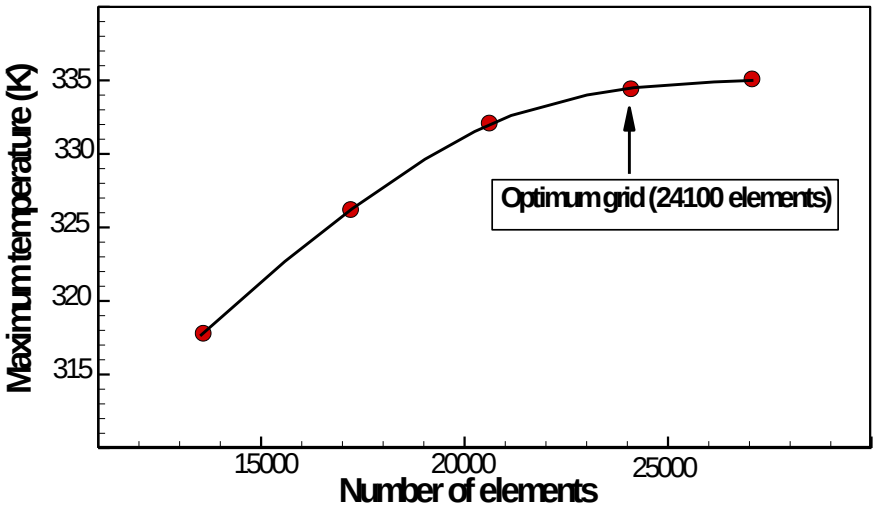

Fig. 2. Calculation of maximum temperature at different mesh sizes

4. Validation

To validate the present numerical simulation and the applied physical model, the SAHs, which were studied experimentally by Chabane et al. [30] and Ramani et al. [31], are simulated and the computed thermal efficiencies are compared with reported experimental data in Fig. 3. Both experimental and theoretical findings show increasing trends for efficiencies of single pass and double pass heaters by increasing the incoming solar heat flux. The effect of air mass flow rate is also studied in Fig. 3-a, for the single-pass SAH, and the positive effect of this parameter on thermal efficiency is observed. Also, it is observed that the maximum value of deviations in thermal efficiencies between the CFD results and experiment are ±4.2% and ±6.1% for the simulated single and double-pass SAHs, respectively.

The result of the present numerical simulation about the flow computation was validated separately with the experimental data reported in Ref. [32]. The natural convection of airflow in a tall enclosure was investigated in that study. The air velocity distribution along the horizontal mid-plane of the enclosure is drawn in Fig. 4, and a comparison is made with the experiment. This figure shows a wide extent of the stagnant zone in the central area and high air velocity near the side walls due to the density gradient. Fig. 4 depicts an acceptable consistency between the current numerical simulation and experiment.

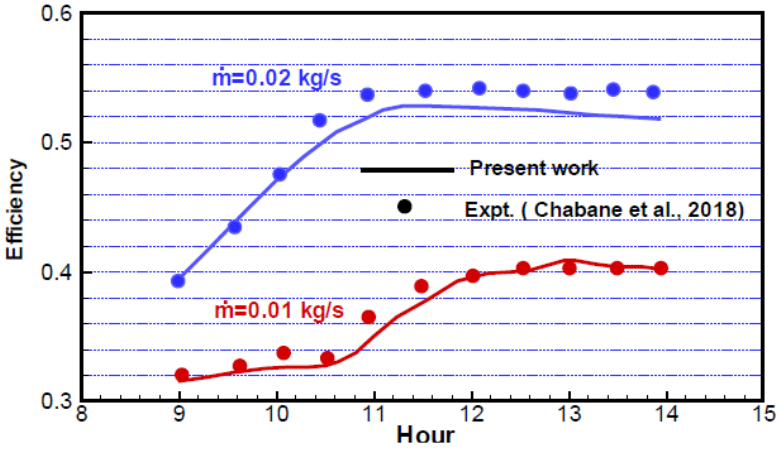

a) Single pass SAH

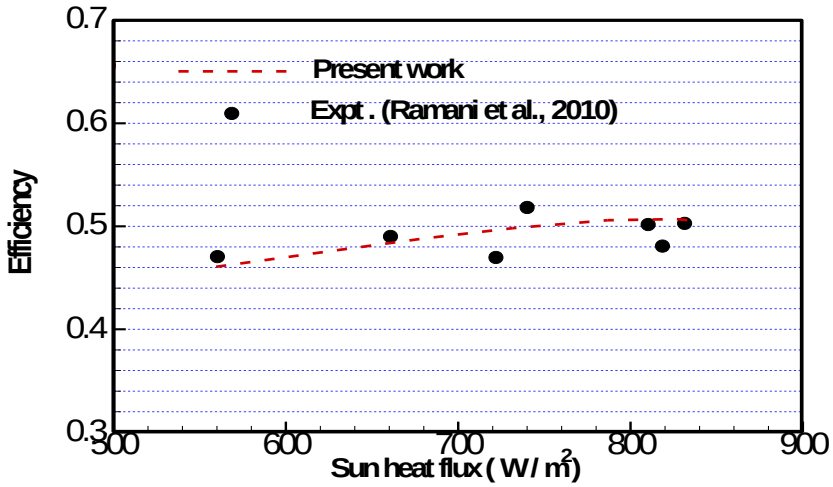

b) Double pass SAH

Fig. 3. Comparison of the computed thermal efficiency for the simulated SAHs with experimental data [30, 31]

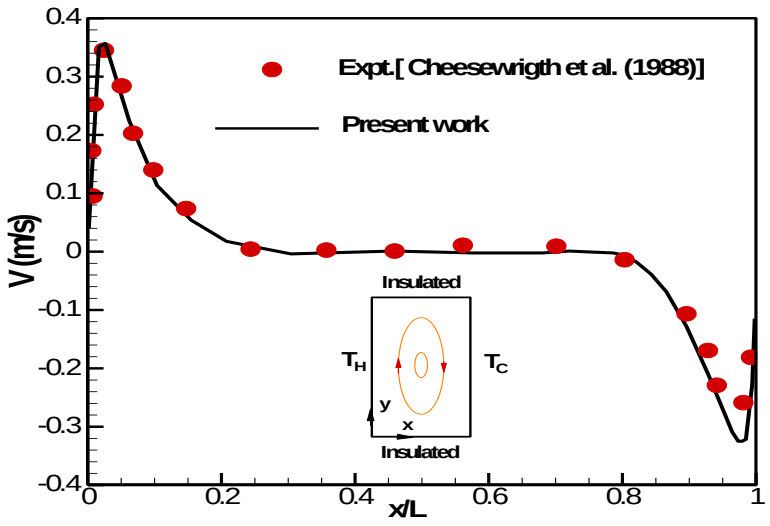

Fig. 4. Velocity distribution at the mid-plane of the enclosure with cold and hot side walls

5. Results

Under the present research work, the effect of the impingement jet on the flow and thermal characteristics of a double pass solar collector with two glass covers is investigated utilizing CFD data from the simulation. All of the following results are obtained with the air mass flow rate of 0.04 kg/s and different solar heat flux in the range of 500 to 1100 W/m^2. At first, to show the airflow pattern inside the heater with jet flows, the contours of velocity magnitude inside the air ducts and jet plate are drawn in Fig. 5. Also, the vector plot of the velocity field for a zoomed region including the second hole in the jet plane is shown in this figure. As noted before, the width of air holes in the jet plate decreases along the flow direction for having an almost equal air mass flow rate for each jet. It is evident that in the case of the same width for each air hole, the last hole at the downstream side will have the maximum jet velocity, which is much higher than the air velocity in the first hole. This behavior will decrease the effect of jet impingement in enhancing convection heat transfer. The high-velocity jet flows moving toward the heated absorber plate are seen in Fig. 5. A recirculated region at the beginning of the air duct above the jet plate, which is due to 180 degrees in the flow direction, happens in the convection flow. The separated zone behaves like a hot region because of the low convection coefficient in this area. The air velocity vector plot shown in Fig. 5 demonstrates the flow pattern inside the jet plate, and also the recirculated flows due to flow separation at the exit section of each air hole are detectable.

The velocity magnitude contours for free convection airflow inside the gap between the two glass covers are drawn in Fig. 6, because of the different order of velocities in forced and free convection flows. The buoyant force due to the density gradient leads to a series of rotating cells which are seen in Fig.6. For having more clear figure for demonstrating the flow pattern in the SAH, the streamline plots for both two convection air flows are depicted in Fig. 7. Several recirculated zones are seen in different parts of the heater duct. Besides, the effect of air jets on flow patterns and also the recirculated cells inside the top air gap can be seen in this figure.

In the air gap between the two glass covers, where the free convection flow is established, and the density gradient is the only driving force, a series of counter-rotating rolls known as the multi-cellular Bénard pattern are observed. This phenomenon is natural convection caused by the buoyancy-driven flow that occurs in a flat horizontal layer of bellow-heated fluid, in which the fluid forms a regular pattern of convective cells, namely Bénard cells or Bénard convection.

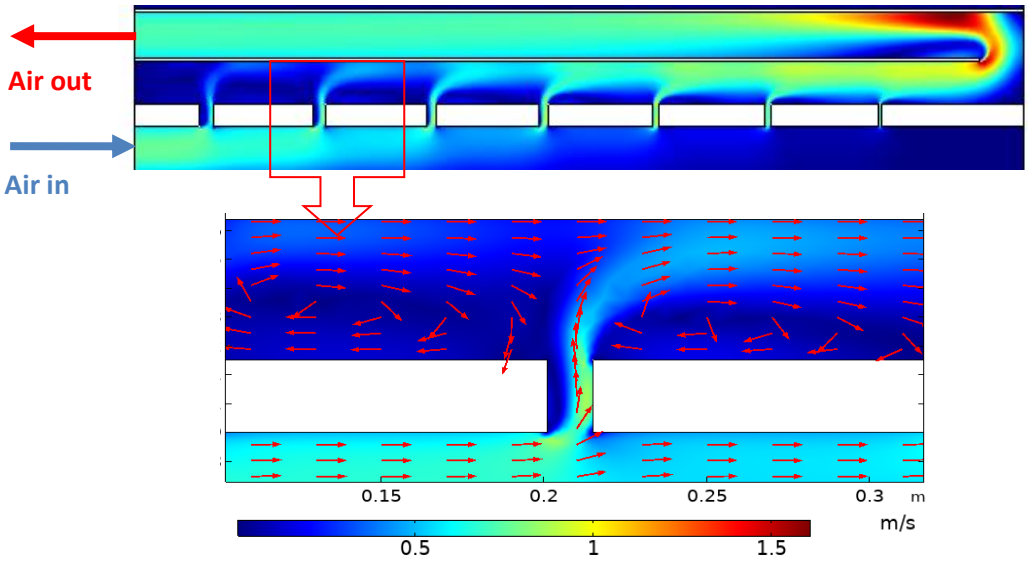

Fig. 5. Contour of air velocity magnitude, $q_{sun} = 800\ W/m^2$

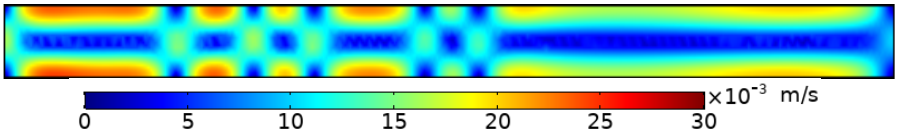

Fig. 6. Contours of velocity magnitude inside the air gap between two glass covers, $q_{sun} = 800\ W/m^2$

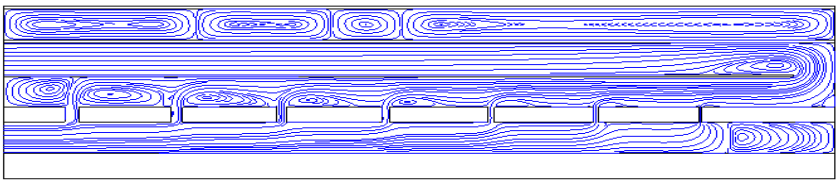

Fig. 7. Streamline plots, $q_{sun} = 800\ W/m^2$

The thermal behavior of the studied double pass SAH is investigated by the temperature contours drawn in Fig. 8. As seen, the maximum temperature belongs to the absorber and the airflow adjacent to this element. As seen, the air jet from the nozzles in the jet plate, which move toward the heated surface, causes flow mixing and increases the heat transfer rate.

The temperature pattern inside an impinging jet is more clearly demonstrated in Fig. 9 by choosing a finite temperature range in plotting contours. As seen, the cold air jet from the nozzle is effectively heated by streaking on the absorber plate, which leads to more convection heat transfer and higher performance.

To investigate the thermal behavior of SAHs with jet impingement, the temperature distribution along the surfaces of glass sheets, absorber, and the insulation layer are plotted in Fig. 10. The absorber surface as the main source of heat transfer has a temperature distribution with decreasing trend along the flow direction. The jet streaking on this surface that leads to a high heat transfer rate is the main factor that causes this thermal behavior, such that in simple SAHs, the temperature distribution along the absorber plate has an increasing trend because of the growing thermal boundary layer along the heated surface. As seen, the lower glass cover has a local maximum temperature at a point upstream of its center, but the upper glass cover and also the insulation layer have almost uniform temperatures along their surfaces, with the average temperature which is not much higher than T_{amb}. The relatively cold outer surfaces of the heater decrease the amount of heat loss and cause higher efficiency.

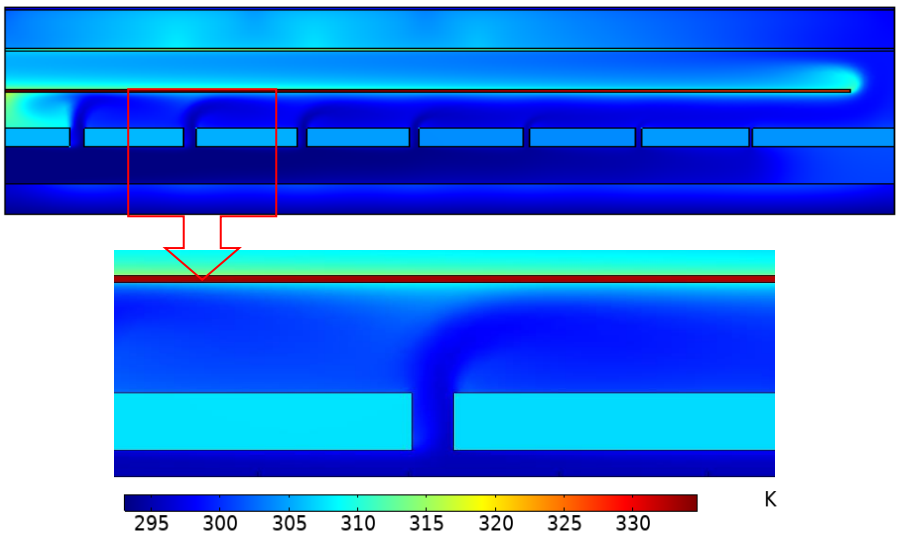

Fig. 8. Temperature contours, $q_{sun} = 800\ W/m^2$

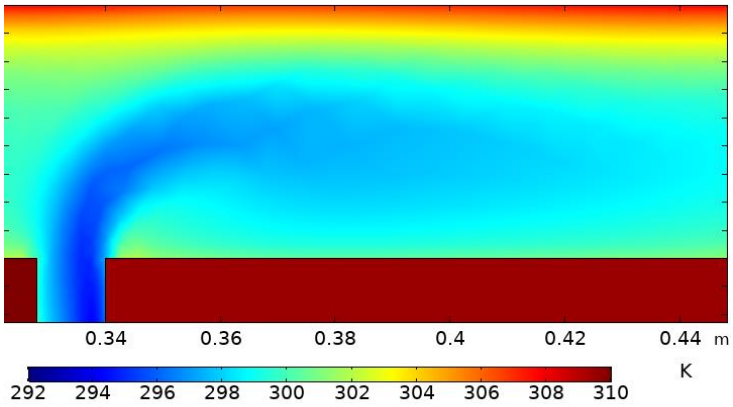

Fig. 9. Temperature contours closed to the nozzle, $q_{sun} = 800\ W/m^2$

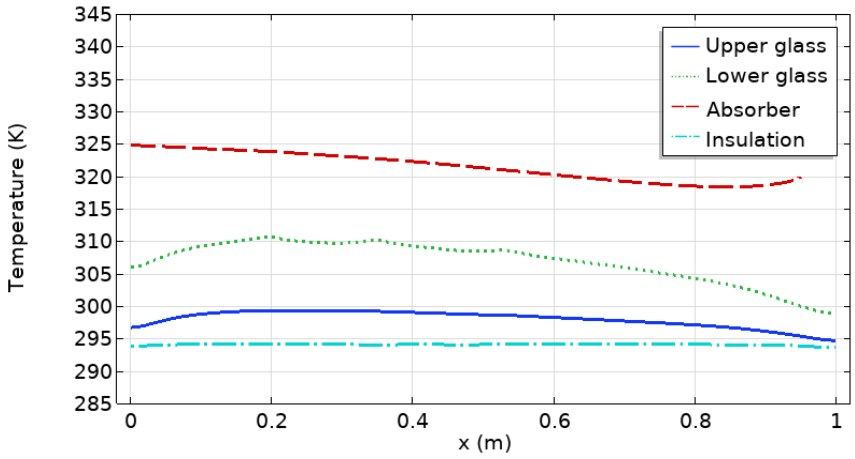

Fig. 10. Temperature variations along different solid parts of SAH, $q_{sun} = 800\ W/m^2$

To demonstrate the effect of solar irradiation on the thermal behavior of the proposed SAH, the temperature contours inside the solar collector and also, the temperature distribution along different parts are drawn in Figs. 11 and 12 at different solar heat fluxes. As expected, the operating temperature of all parts of SAH increases with the value of incoming solar heat flux. Figure 11, shows hot regions inside the recirculated domain, for example, above the beginning of the jet plate and also on the separated zone above the downstream side of the absorber.

The curves drawn in Fig. 12 show increasing trends for glass cover, absorber, and insulation layer temperatures as the solar heat flux get higher values. From these elements, the most sensitive temperature against solar irradiation belongs to the absorber, on which temperature decreases along the flow direction due to the high convection coefficient between the cold air jets and the heated surface and the high rate of mixing process close to the absorber.

In Fig. 13, the temperature distributions across the SAH along the vertical line at x=0.45 m are drawn at two different solar heat fluxes. This figure can show how the airflow is heated via the convection heat transfer with the heated surface. The maximum temperature belongs to the absorber and the minimum for the insulation layer. The wavy form of temperature variation above the jet plate is due to the high rate of flow mixing between the jet and the main airflow in the duct of the heater. It is worth mentioning that the air temperature increase close to the lower glass is due to surface radiation with the high-temperature absorber surface that causes a considerable incoming radiative heat flux toward the glass.

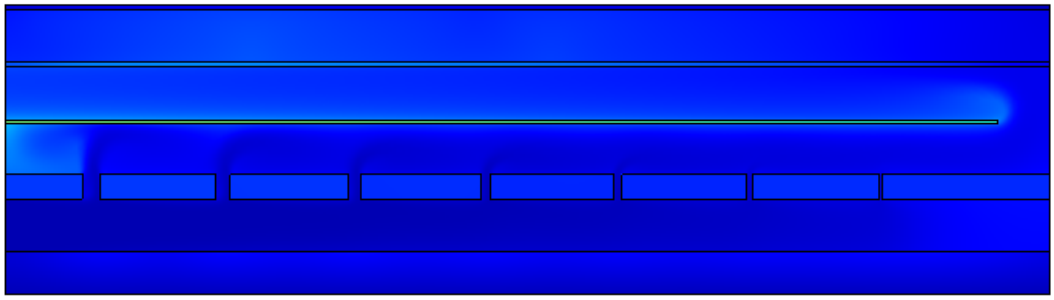

a) $q_{sun} = 500\ W/m^2$

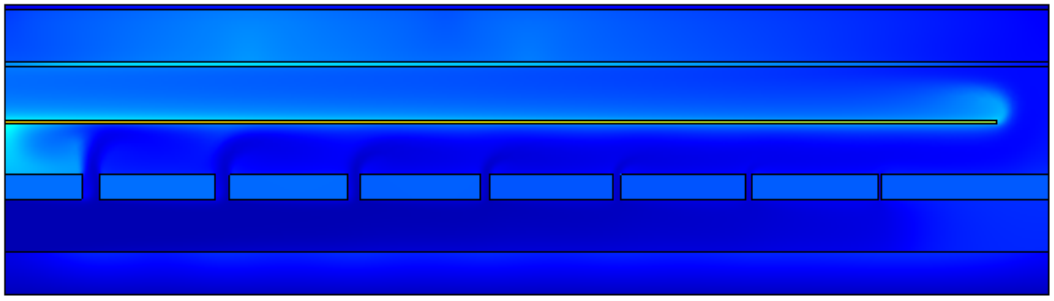

b) $q_{sun} = 700\ W/m^2$

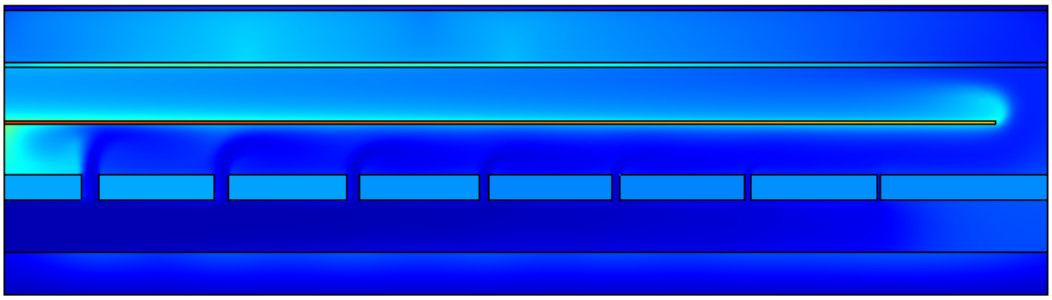

c) $q_{sun} = 900\ W/m^2$

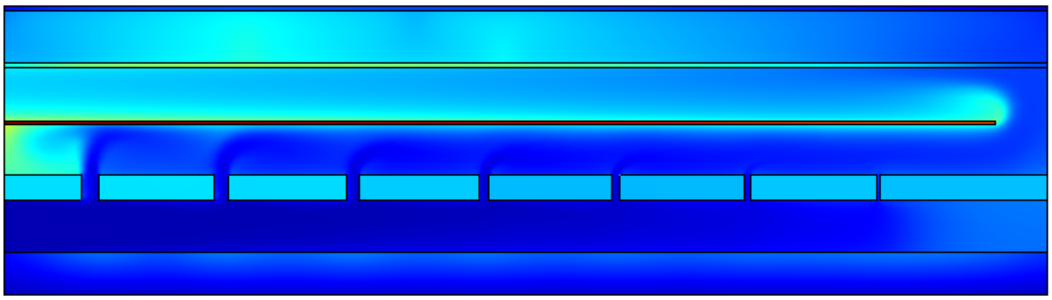

d) $q_{sun} = 1100\ W/m^2$

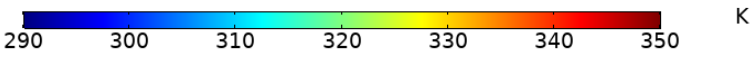

Fig. 11. Effect of solar irradiation on temperature field m=0.04kg/s(V_{in}=0.7m/s)

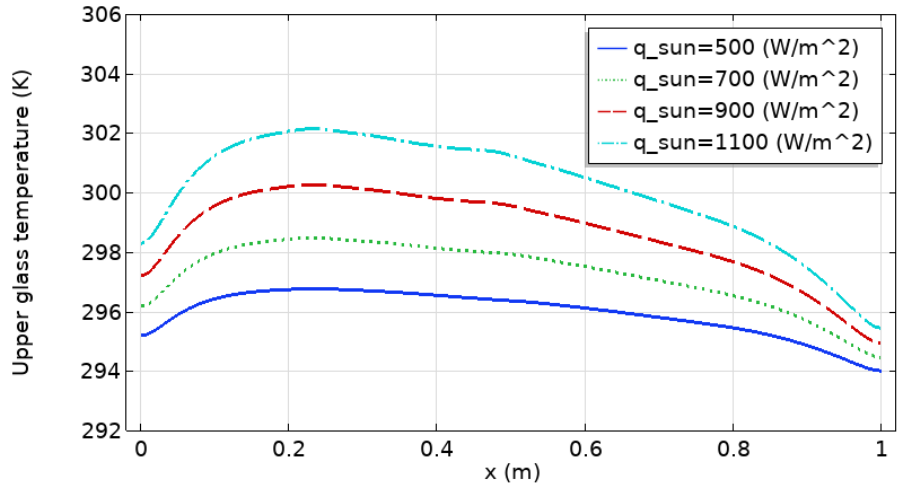

a) Upper glass cover

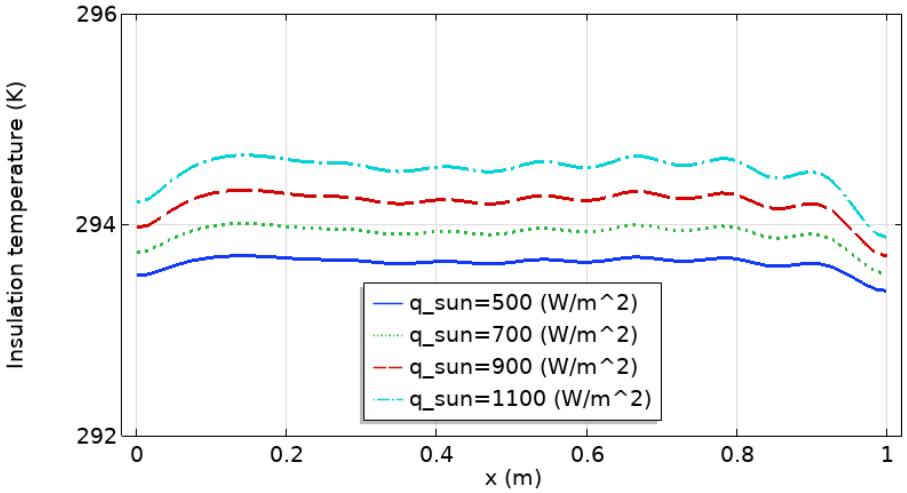

b) Insulation

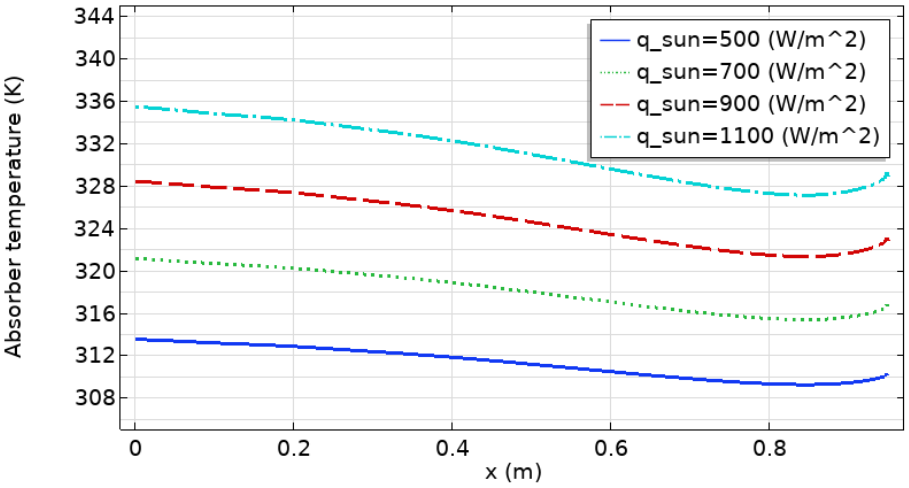

c) Absorber

Fig. 12. Temperature distributions along different parts of SAH

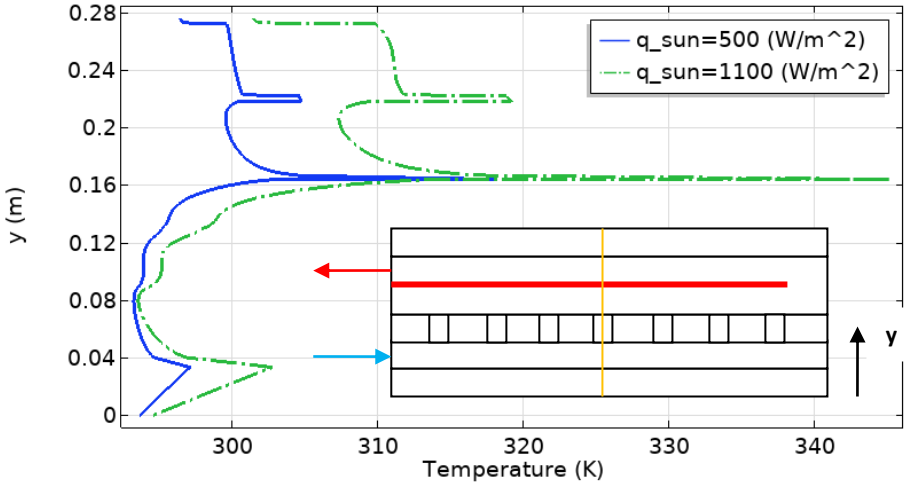

Fig. 13. Temperature distribution across the SAH

The main parameter of SAH is thermal efficiency, which shows the ability of the heater to energy conversion between solar radiation into gas enthalpy. The variation of SAH efficiency as a function of solar heat flux at two different mass flow rates is depicted in Fig. 14. This figure demonstrates an increasing trend for thermal efficiency as the mass flow rate gets a higher value. Also, a slight decrease in the value of thermal efficiency is seen by increasing in solar irradiation. Besides, a comparison is made between the performances of double SAH with jet impingement and a simple one without a jet plate. As shown, at different values of air mass flow rate and also the incoming solar heat flux, the jet impingement technique proves well its role in enhancing heat transfer and increasing thermal efficiency. Such that the percentage of efficiency increase for the two examined mass flow rates of 0.04 and 0.02 kg/s is about 5.7% and 10%, respectively.

Since the double pass SAHs without a jet plate is also simulated in the present work, the thermohydrodynamic characteristics of this type of air heater is presented here by plotting the velocity magnitude and temperature contours at $\dot{m} = 0.04\ kg/s, q_{sun} = 1100\ W/m^2$.

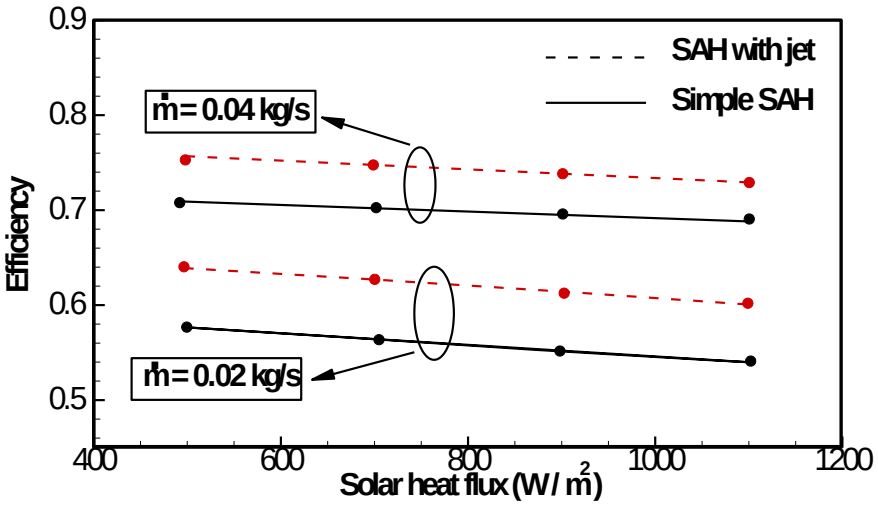

Fig. 14. Variation of efficiency with the solar heat flux at different air mass flow rate

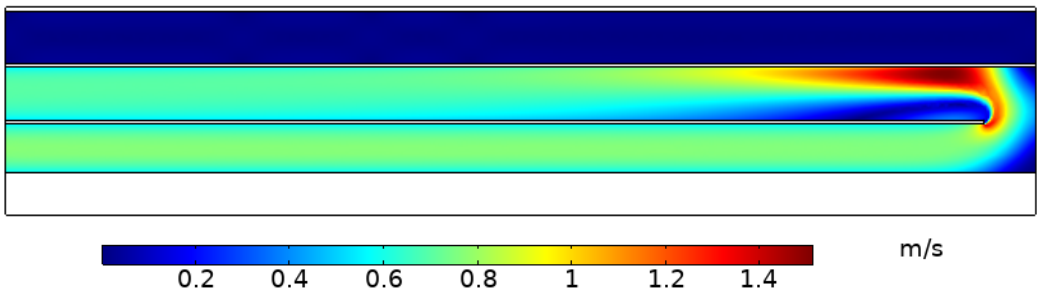

a) Contours of velocity magnitude

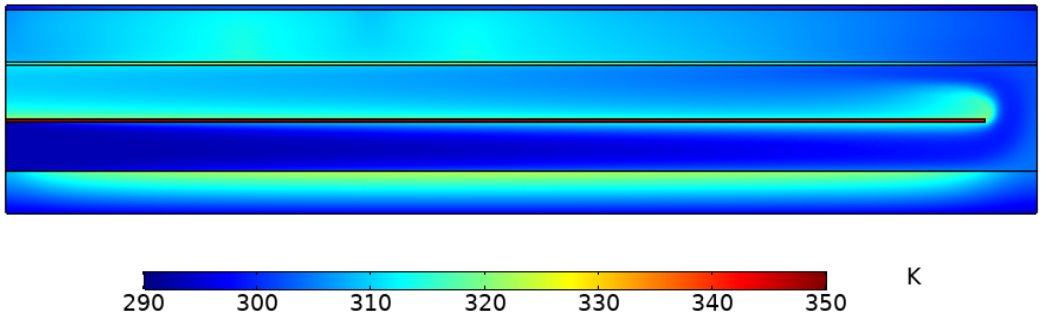

b) Temperature contours

Fig. 15. Temperature and velocity magnitude contour plots

Comparison between Figs. 15-a and b with similar ones presented for SAH with the jet plate can show the positive effect of jet impingement on improving the heater performance. Such that the heat propagation from the absorber surface into the streaking convective airflow to the absorber is much higher and the growth of thermal boundary layer that happens in simple SAH vanishes due to flow mixing and turbulence generation by the jet flows.

6. Concluding remarks

In double pass two glazed SAHs, the rate of heat loss from the glass cover decreases because the heated absorber plate is kept away from the cold ambient. For this type of collector, it is expected that employing the jet impingement technique in which the absorber is located above the jet plate can lead to considerable performance improvement. So, the effect of this technique on the thermal performance of double pass, two glazed SAHs is examined for the first time by the CFD method, and this combination is expected to lead to an efficient solar system. For this, the flow equations for both turbulent forced convection inside the heater ducts and free convection airflow between two glass sheets are solved by employing the RNG k–ε turbulence model. The Laplace equation is also solved in the insulation layer, glass sheets, jet plate, and absorber. The numerical finding revealed the positive effect of jet impinging on the efficiency of SAH under all considered different operating conditions. Comparison between the efficiencies of jet SAH with a convention type at the two air mass flow rates of 0.02 and 0.04 kg/s showed about 10% and 5.7% increase in thermal efficiencies, respectively, due to using the jet plate in the construction of the heater.

References

[1] M. Aramesh, M. Ghalebani, A. Kasaeian, H. Zamani, G. Lorenzini, O. Mahian, S. Wongwises, A review of recent advances in solar cooking technology, Renew. Energy. 140 (2019) 419–435. doi:10.1016/j.renene.2019.03.021.

[2] S. A. Kalogirou, Solar thermal collectors and applications, Progress in Energy and Combustion Science, 30 (2004) 231–295. doi:10.1016/j.pecs.2004.02.001.

[3] A.P. Singh, O.P. Singh, Thermo-hydraulic performance enhancement of convex-concave natural convection solar air heaters, Sol. Energy. 183 (2019) 146–161. doi:10.1016/j.solener.2019.03.006.

[4] S. Singh, Experimental and numerical investigations of a single and double pass porous serpentine wavy wiremesh packed bed solar air heater, Renew. Energy. 145 (2020) 1361–1387. doi:10.1016/j.renene.2019.06.137.

[5] M. Nemś, J. Kasperski, Experimental investigation of concentrated solar air-heater with internal multiple-fin array, Renew. Energy. 97 (2016) 722–730. doi:10.1016/j.renene.2016.06.038.

[6] B. K. Gandhi, K. M. Singh, Experimental and numerical investigations on flow through wedge shape rib roughened duct, Journal of the Institution of Engineers (India): Mechanical Engineering Devision, 90 (2010) 13-18. doi.org/10.1007/s00231-016-1822-5

[7] M. Foruzan Nia, S.A. Gandjalikhan Nassab, A.B. Ansari, Numerical Simulation of Flow and Thermal Behavior of Radiating Gas Flow in Plane Solar Heaters, J. Therm. Sci. Eng. Appl. 12 (2020) 1–8. doi:10.1115/1.4044756.

[8] A.D. Rayeni, S.A.G. Nassab, Effects of Gas Radiation on Thermal Performances of Single and Double Flow Plane Solar Heaters, Int. J. Eng. 33 (2020) 1156–1166. doi:10.5829/ije.2020.33.06c.14.

[9] Y. Sheikhnejad, S. A.Gandjalikhan Nassab, Enhancement of solar chimney performance by passive vortex generation , Renewable Energy, 169 (2021) 437-450. doi.org/10.1016/j.renene.2021.01.026

[10] S. A. Gandjalikhan Nassab, Efficient design of converged ducts in solar air heaters for higher performance, Heat and Mass Transfer, 2023 (59), 363-375, https://doi.org/10.1007/s00231-022-03228-9

[11] J. Hu, K. Liu, L. Ma, X. Sun, 2018. Parameter optimization of solar air collectors with holes on baffle and analysis of flow and heat transfer characteristics. Sol. Energy 2018(174) 878-889, https://doi.org/10.1016/j.solener.2018.09.075.

[12] T. Brown, 1968. Evaluation of internal heat transfer coefficients for impingement cooled turbine airfoils. Journal of Aircraft, 1968 (6), 203-214, doi.org/10.2514/3.44036.

[13] W. C. Tan, L. H. Saw, H. S. Thiam, J. Xuan, Z. Cai, M. C. Yew, Overview of porous media/metal foam application in fuel cells and solar power systems. Renew. Sustain. Energy Rev. 2018(96) , 181–197. doi.org/10.1016/j.rser.2018.07.032.

[14] C.Choudhury, H. P.Garg, Evaluation of a jet plate solar air heater. Sol. Energy 46 (4)(1991) 199–209. https://doi.org/10.1016/0038-092X(91)90064-4.

[15] M. Belusko, W. Saman, F.Bruno,Performance of jet impingement in unglazed air collectors Sol. Energy 82 (5)(2008) 389–398. https://doi.org/10.1016/j.solener.2007.10.005

[16] Y. Xing, S. Spring, B. Weigand, Experimental and numerical investigation of heat transfer characteristics of inline and staggered arrays of impinging jets. J. Heat Transf. 132 (9) (2010) 1–11. https://doi.org/10.1115/1.4001633.

[17] M. Zukowski, Heat transfer performance of a confined single slot jet of air impinging on a flat surface. Int. J. Heat Mass Transf. 57 (2) (2013) 484–490. https://doi.org/10.1016/j.ijheatmasstransfer.2012.10.069.

[18] M. Zukowski, Experimental investigations of thermal and flow characteristics of a novel microjet air solar heater. Appl. Energy 142 (2015), 10–20. doi.org/10.1016/j. apenergy.2014.12.052.

[19] R. Chauhan, N. S. Thakur, Investigation of the thermohydraulic performance of impinging jet solar air heater. Energy 2014(68), 255–261. doi.org/10.1016/j.energy.2014.02.059.

[20] R. Chauhan, T. Singh, N. S. Thakur, A. Patnaik,. Optimization of parameters in solar thermal collector provided with impinging air jets based upon preference selection index method. Renew. Energy 2016(99), 118–126. doi.org/10.1016/j.renene.2016.06.046.

[21] M. M. Matheswaran, T. V. Arjunan, D. Somasundaram, Analytical investigation of solar air heater with jet impingement using energy and exergy analysis. Sol. Energy. 2018, doi.org/10.1016/j.solener.2017.12.036.

[22] T. Rajaseenivasan, S. Ravi Prasanth, M. Salamon Antony, K. Srithar, Experimental investigation on the performance of an impinging jet solar air heater. Alexandria Eng. J. 56 (1) (2017) 63–69. https://doi.org/10.1016/j.aej.2016.09.004

[23] S. Yadav, S. P. Saini, Numerical investigation on the performance of a solar air heater using jet impingement with absorber plate, Solar Energy (208), (2020) 236-248, https://doi.org/10.1016/j.solener.2020.07.088

[24] A. M. Aboghrara, B.T. H.T.Baharudin, M.A. Alghoul, K. Sopian, N. M. Adam, A. A. Hairuddin, Performance Analysis of Single Pass Solar Air Heater with Jet Impingement on Wavy Shape Corrugated Absorber Plate, Case Studies in Thermal Engineering, 2017 (23), 124-135, doi.org/10.1016/j.csite.2017.04.002

[25] H. M. Abd,O. R. Alomar, M. M. Mohamed Salih, Improving the performance of solar air heater using a new model of V-corrugated absorber plate having perforations jets, 2022 (46), 8130-9144, doi.org/10.1002/er.7715

[26] R. Chauhan , T.Singh , N.S. Thakur, A. Patnaik, Optimization of parameters in solar thermal collector provided with impinging air jets based upon preference selection index method, Renewable Energy, 2016 (99), 116-126, doi.org/10.1016/j.renene.2016.06.046

[27] F. P. Incropera, D. P. De Witt, Introduction to heat transfer, Forth Edittion (2002), John Wiley and Sons, Newyork.

[28] B. E. Launder, D. B.Spalding, The numerical computation of turbulent flows, Computer methods in applied mechanics and engineering, 3(2) (1974) 269-289. doi.org/10.1016/0045-7825(74)90029-2

[29] A.P. Singh, Akshayveer, A. Kumar, O.P. Singh, Designs for high flow natural convection solar air heaters, Sol. Energy. 193 (2019) 724–737. doi:10.1016/j.solener.2019.10.010.

[30] F. Chabane, M. Noureddine, A. Brima, Experimental study of thermal efficiency of a solar air heater with an irregularity element on absorber plate, International Journal of Heat and Technology, 36,(2018) 855-860. doi:10.18280/IJHT.360311

[31] B. M. Ramani, A. Gupta, R. Kumar, Performance of a double pass solar air collector, Solar Energy, 84, (2010) 1929-1937. doi:10.1016/j.solener.2010.07.007

[32] R. Cheesewright, K. J. King, S. Ziai (1986), Experimental data for the validation of computer codes for the prediction of two-dimensional buoyant cavity flows. Significant questions in buoyancy affected enclosure or cavity flows, HTD-60, ASME Winter Annual Meeting, Anaheim, December 1986, 75.